Journal of Beijing Institute of Technology, 2024, Vol. 33, No. 3

Microwave Through Wall Imaging via An Induced Current Learning Method

Pengjin Lan, Jianguo Huang, Tianyi Zhou✉

Abstract: In this paper, an induced current learning method (ICLM) for microwave through wall imaging (TWI), named as TWI-ICLM, is proposed. In the inversion of induced current, the unknown object along with the enclosed walls are treated as a combination of scatterers. Firstly, a non-iterative method called distorted-Born backpropagation (DB-BP) is utilized to generate the initial result. In the training stage, several convolutional neural networks (CNNs) are cascaded to improve the estimated induced current. In addition, a hybrid loss function consisting of the induced current error and the permittivity error is used to optimize the network parameters. Finally, the relative permittivity images are conducted analytically using the predicted current based on ICLM. Both the numerical and experimental TWI tests prove that, the proposed method can achieve better imaging accuracy compared to traditional distorted-Born iterative method (DBIM).

Keywords: through wall imaging; inverse scattering problem; convolutional neural network (CNN)

1 Introduction

By levering of microwave signal, microwave through wall imaging (TWI) focuses on detecting the position, shape and the constitutive parameters of targets behind the obstacles. Due to its penetration properties, microwave TWI has significant practical applications in many fields [1–3], such as military monitoring, non-destructive testing and biomedical imaging.

As an important branch of inverse scattering problem (ISP), microwave TWI can be considered as an inhomogeneous ISP with bounded background. Due to the multiple scattering between the wall and the object, the ill-posedness and nonlinearity of ISP with inhomogeneous background are further increased significantly, making inversion more difficult than in homogeneous scenarios. To address such problems, a straightforward solution is to transform the inhomogeneous ISP into a homogeneous one by introducing the inhomogeneous background Green's function, with the related methods such as the distorted-Born iterative method (DBIM) [4]. However, the calculation of the Green's functions leads to additional computational costs. To improve the inversion efficiency, a new integral equation is developed for the inhomogeneous background ISP [5].

Recently, thanks to its powerful non-linear fitting capabilities, deep learning has been widely used for the solving of ISP [6–12]. In terms of imaging speed and quality, learning-based methods have been shown to outperform traditional algorithms. In [6], three inversion schemes are proposed to reconstruct the permittivity from different input data, including directly from raw scattering field data, rough images derived from dominant current and backpropagation (BP). Furthermore, convolutional neural networks (NNs) are employed to imitate the iterations of

Manuscript received Mar. 14, 2024; revised Mar. 30, 2024; accepted Apr. 18, 2024. The associate editor coordinating the review of this manuscript was Dr. Xiuzhu Ye. This work was supported by the National Natural Science Foundation of China (No. 62101288).

Pengjin Lan, Jianguo Huang and Tianyi Zhou are with Faculty of Electrical Engineering and Computer Science, Ningbo University, Ningbo 315211, China.

✉ Corresponding author. Email: zhoutianyi@nbu.edu.cn

DOI: 10.15918/j.jbit1004-0579.2024.037

the Born iterative method (BIM) [8]. The problem of TWI was also solved by using deep learning. In [9], a roughly estimated image of unknown scatterers embedded in an inhomogeneous background is recovered by distorted-Born backpropagation (DB-BP), which is enhanced by generative adversarial network.

In this paper, we present an induced current learning method (ICLM) for the microwave TWI. The input of network is taken as the induced current and the raw permittivity image obtained from DB-BP. In the learning of induced current, the unknown object along with the enclosed walls are treated as a combination of scatterers. Taking use of the predicted induced current by network, the permittivity image is conducted based on an analytical solution. To improve the reliability of the inversion, we define a hybrid loss function composed of the induced current error and the permittivity error to guide the learning process. The proposed TWI-ICLM is both verified with synthetic examples and experimental data to demonstrate its superiority over traditional inversion method.

2 Forward Problem

In a 2-D bounded domain of interest D, as depicted in Fig. 1, the unknown object with relative permittivity ε_{obj} is surrounded by the enclosed wall of relative permittivity $\varepsilon_{\text{wall}}$. There

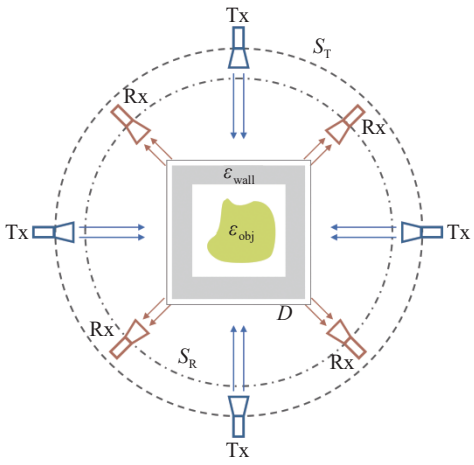

Fig. 1 The TWI setups based on typical configuration of ISP

are N_i transmitters (Tx) located on the circle S_T illuminate the scatterer. To collect the echo signal, the scattered field excited by each incidence is measured by N_r receivers (Rx) located on S_R.

The forward problem involves calculating the scattered field with known permittivity of scatterers. We discretize the domain D into $M \times M$ subunits, and use the method of moments (MoM) to calculate the scattered field. The discretized Lippmann–Schwinger equation can be expressed as

$$\boldsymbol{E}^{\text{t}} = \boldsymbol{E}^{\text{i}} + \boldsymbol{G}_{\text{D}}\boldsymbol{J} \tag{1}$$

where $\boldsymbol{E}^{\text{t}}$ and $\boldsymbol{E}^{\text{i}}$ indicate the total field and incident field, respectively. $\boldsymbol{G}_{\text{D}}$ is the free-space Green's function mapping each units of domain D. The induced current $\boldsymbol{J}$ is defined as $\boldsymbol{J} = \boldsymbol{\chi}\boldsymbol{E}^{\text{t}}$, where $\boldsymbol{\chi}(r) = \boldsymbol{\varepsilon}(r) - 1$ is the contrast function, where $\boldsymbol{\varepsilon}(r)$ is the relative permittivity at r in domain D. As reradiation of the induced current, the scattered field $\boldsymbol{E}^{\text{s}}$ can be calculated by

$$\boldsymbol{E}^{\text{s}} = \boldsymbol{G}_{\text{S}}\boldsymbol{J} \tag{2}$$

where $\boldsymbol{G}_{\text{S}}$ is the Green's function which represents the mapping relation between the induced current and the scattered field. In contrary to the forward problem, the problem of inverse scattering is to retrieve the permittivity distribution of unknown scatterer in the interested domain D.

3 Method

The flowchart of the proposed TWI-ICLM is shown in Fig. 2. Considering the TWI as an ISP with inhomogeneous background, the inducted current $\boldsymbol{J}_{\text{obj}}^{\text{db-pb}}$ and preliminary reconstruction result $\boldsymbol{\varepsilon}_{\text{obj}}^{\text{db-bp}}$ of the object is generated by a distorted-Born approximation method based on backpropagation scheme, i.e. DB-BP. More methodologies details of DB-BP can be found in [9]. Unlike using dominant current as the initialization [7], the induced current is directly adopted as the starting point of the learning for the simplification of computation. To incooperate more prior information, the input of CNN

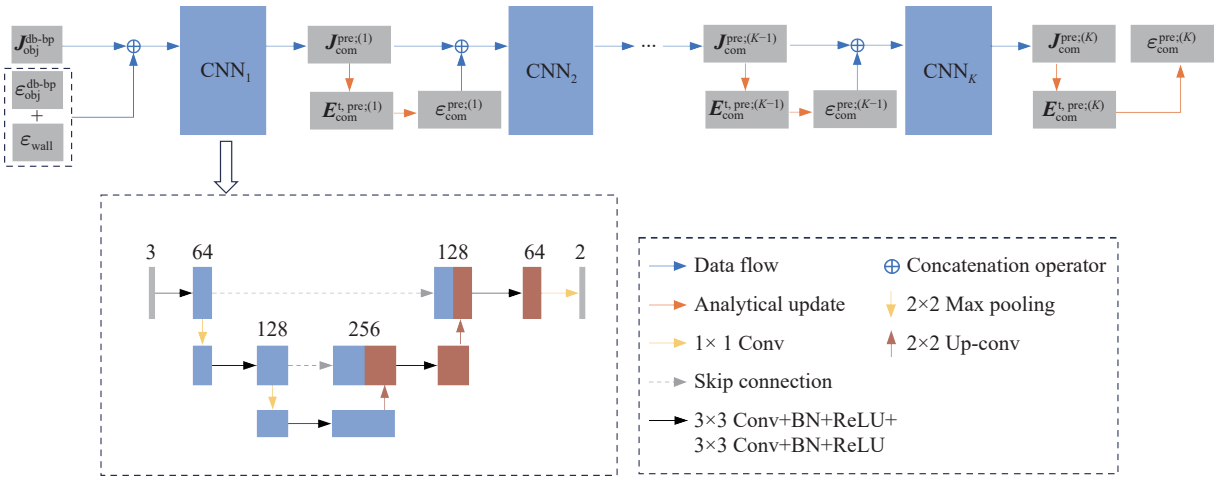

Fig. 2 Overall flowchart of the proposed TWI-ICLM.

adopts the concatenation of the current $\boldsymbol{J}_{\text{obj}}^{\text{db-bp}}$ and the permittivity of object and wall $\boldsymbol{\varepsilon}_{\text{com}}$, where $\boldsymbol{\varepsilon}_{\text{com}}$ is calculated as the sum of $\boldsymbol{\varepsilon}_{\text{obj}}^{\text{db-b}p}$ and $\boldsymbol{\varepsilon}_{\text{wall}}$. To effectively regress the induced current, a total of K CNNs are cascaded for training. The cascaded number K can be adjusted according to the complexity of the problem. In this paper, the cascaded number is set as 4. It is worth to note that the object and the wall together is considered as a combination, so the variables with the subscript "com" in the following text indicate the physical quantities of the combination.

In the learning process, each CNN updates the predicted current $\boldsymbol{J}_{\text{com}}^{\text{pre}}$, then the total field $\boldsymbol{E}_{\text{com}}^{\text{t,pre}}$ can be derived from (1). According to the relationship between induced current and total field, for the p-th incidence, each element of the predicted contrast $\boldsymbol{\chi}_{\text{com}}^{\text{pre}}(n)$ at n-th grid can be calculated by

$$\boldsymbol{\chi}_{\text{com}}^{\text{pre}}(n)=\frac{\sum_{p=1}^{N_i}\boldsymbol{J}_{\text{com}}^{\text{pre}}(n)\left[\boldsymbol{E}_{\text{com}}^{\text{t,pre}}(n)\right]^*}{\sum_{p=1}^{N_i}\left\|\boldsymbol{E}_{\text{com}}^{\text{t,pre}}(n)\right\|^2} \tag{3}$$

Based on the definition of contrast function, the permittivity image $\boldsymbol{\varepsilon}_{\text{com}}^{\text{pre}}$ can be reconstructed finally.

Furthermore, a hybrid loss function constructed with the errors of both induced current and permittivity is taken to update the weights of the network. The loss function is defined as

$$\text{Loss}=L_{\text{J}}+w_1L_{\text{MSE}}+w_2L_{\text{SSIM}} \tag{4}$$

where w_γ ($\gamma=1,2$) are weights and L_{J} represents the reconstruction error of the induced current. L_{MSE} is the mean square error (MSE) which checks the distance between the predicted and the actual permittivity. The structural similarity (SSIM) loss L_{SSIM} measures the perceptual distance of two permittivity images. Specifically, each loss function is defined as

$$L_{\text{J}}=\frac{1}{N_i}\sum_{p=1}^{N_i}\left\|\boldsymbol{J}_{\text{com},p}^{\text{true}}-\boldsymbol{J}_{\text{com},p}^{\text{pre}}\right\|^2 \tag{5}$$

$$L_{\text{MSE}}=\left\|\boldsymbol{\varepsilon}_{\text{com}}^{\text{true}}-\boldsymbol{\varepsilon}_{\text{com}}^{\text{pre}}\right\|^2 \tag{6}$$

$$L_{\text{SSIM}}=1-\text{SSIM}(\boldsymbol{\varepsilon}_{\text{com}}^{\text{true}},\boldsymbol{\varepsilon}_{\text{com}}^{\text{pre}}) \tag{7}$$

where $\boldsymbol{J}_{\text{com}}^{\text{true}}$ and $\boldsymbol{\varepsilon}_{\text{com}}^{\text{true}}$ are the corresponding label variables, respectively.

4 Numerical and Experimental Results

In this section, effectiveness of the proposed TWI-ICLM is verified both synthetic and experimental data. The performance of the TWI-ICLM is compared with typical DBIM method. For fair comparison, DBIM is also initialized by DB-BP.

4.1 Inversion with Synthetic Data

In the numerical experiments, the operating frequency is set as 2.4 GHz. There are 12 transmitters and 24 receivers distributed around a circle

of radius 4.54λ. The size of investigation domain D is $2\lambda \times 2\lambda$, which is discretized into 60×60 pixels. The relative permittivity of enclosed square wall is set to 2.

Firstly, 5 000 scatterers modeled by digital objects from the MNIST dataset are chosen for the network training. The relative permittivity of all the digital scatterers is set between 2 and 3. Adam optimizer is adopted in the optimization and its hyper parameters are set to default. Initial learning rate is set to 0.000 2, and it decays 20% every 8 epochs. The loss weights w_1 and w_2 are all set to 2.

The reconstruction results of three representative examples are shown in Fig. 3. The corresponding quantitative evaluation metrics are summarized in Tab. 1. All testing samples are added with additive white Gaussian noise, which has a signal-to-noise ratio (SNR) of 15 dB. It can be seen obviously from Fig. 3 and Tab. 1, the reconstructions of the TWI-ICLM are much better than DBIM method. Quantitatively, the images reconstructed by DBIM are rather rough with many artefacts. In comparison, the relative permittivity profiles are successfully reconstructed by TWI-ICLM. Furthermore, the predicted induced current and its reference is shown in Fig. 4. It is proven that the proposed method can also reconstruct the induced current accurately.

4.2 Experimental verification

In order to further verify the proposed TWI-ICLM, the test of cylindrical object inside enclosed wall is carried out with experimental data. As shown in Fig. 5, the experiment was conducted by a 2-D microwave TWI system previously reported in [13]. The 2.4 GHz system is polarized as transverse magnetic and there are 24 antennas evenly distributed on a circumference of radius 4.54λ. One of antennas is works as the transmitter and the rest are acted as the receiver. In the experimental implementation, the object is first placed to its initial position, and then the measurement is performed by a vector network

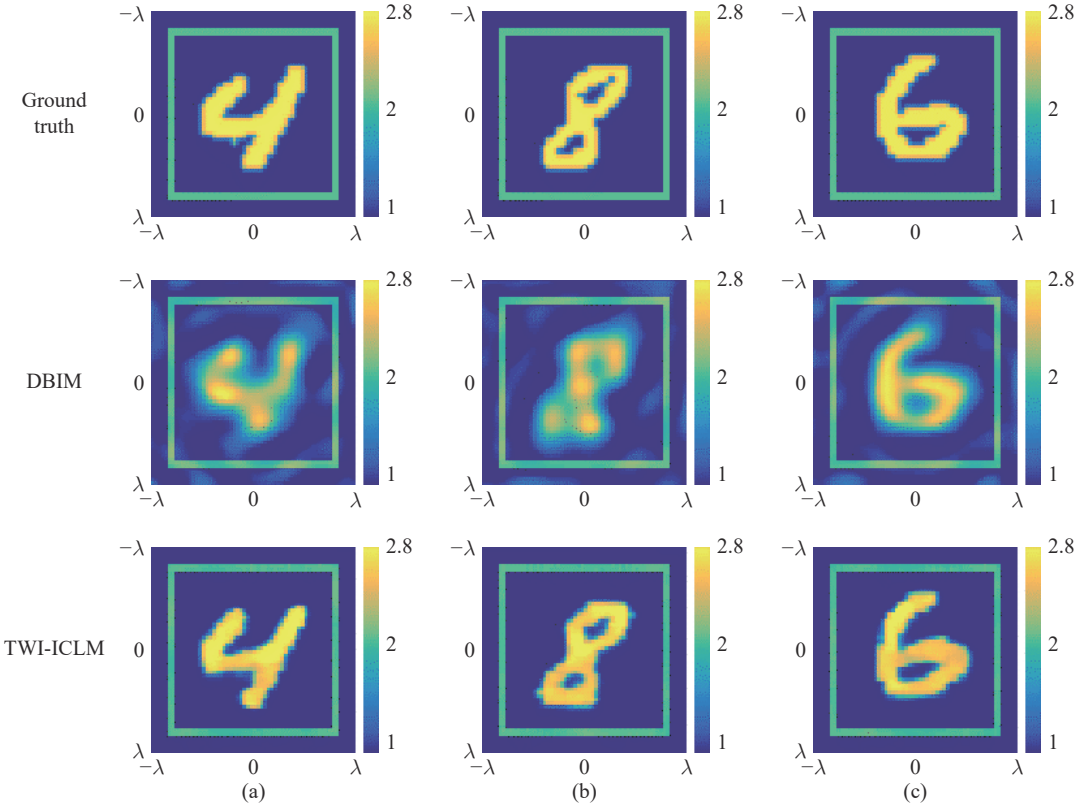

Fig. 3 Reconstruction results of Test 1–Test 3 from the MNIST dataset: (a) Test 1; (b) Test 2; (c) Test 3

analyzer (VNA). After the finish of the VNA mearing, the turn table was rotated by 30 degree for the next measurement with different incidence. Such rotating and measurement were repeated 11 times to accomplish a 12 × 23 matrix containing measured scattered field. Before the inversion, the measured data is calibrated using the same method as referred in [13].

Fig. 6 (a) shows the exact configuration of two TWI experimental cases. The wall is made of

Tab. 1 MSES/SSIM for the reconstructions in Fig. 3

Method	Test 1	Test 2	Test 3
DBIM	0.067/0.763	0.070/0.723	0.054/0.782
TWI-ICLM	0.026/0.940	0.018/0.956	0.025/0.941

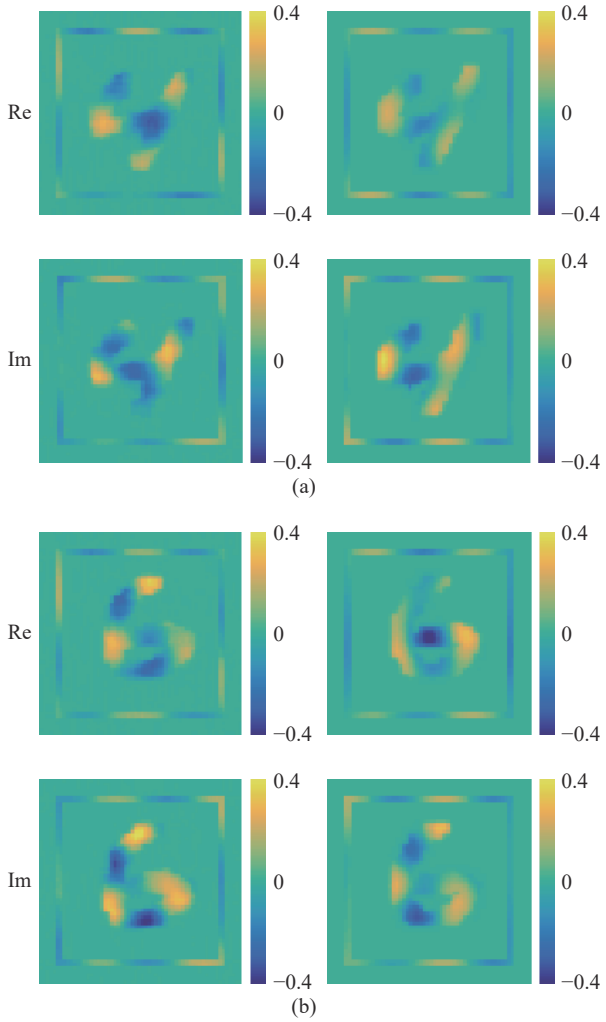

Fig. 4 Retrieved induced currents of Test 1 and Test 3 for a certain incidence. For each test, the left and right columns are the output induced current of TWI-ICLM and the label induced current: (a) Test 1; (b) Test 3

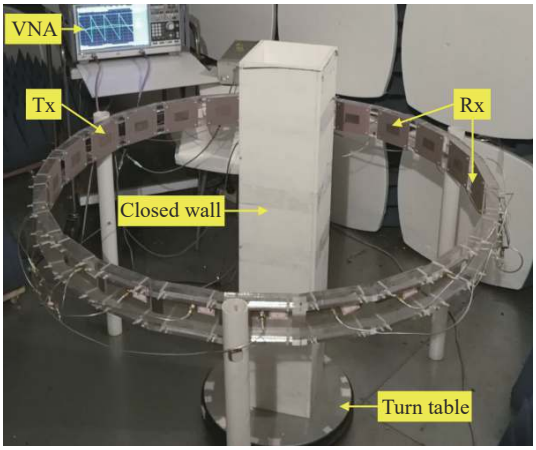

Fig. 5 Photograph of experimental system

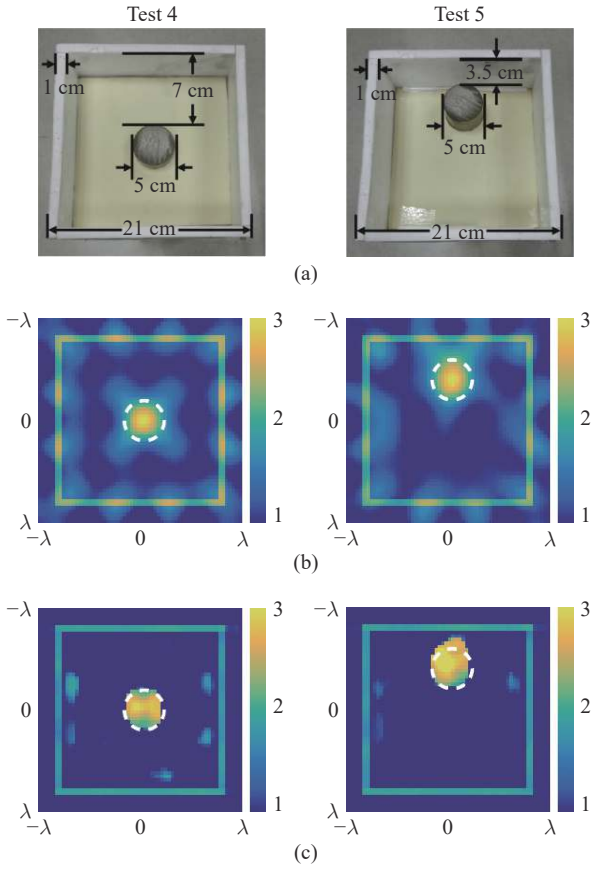

Fig. 6 Reconstruction results of experimental data: (a) ground-truth images for two TWI examples; (b) reconstructed image using DBIM; (c) reconstructed image using TWI-ICLM

Teflon with a permittivity of 2. The object is a cylinder with a diameter of 5 cm and the permittivity of 3. The reconstructed results of DBIM and TWI-ICLM are shown in Fig. 6 (b) and (c), respectively. Practically, the network was retrained by a new dataset consisting of 5 000

cylindrical scatters with random relative permittivity, radius, number, and position. The radius between 0.15λ and 0.25λ, and the number is between 1 and 2. The relative permittivity range of all cylinders is between 2.5 and 3.3.

It can be seen from Fig. 6 (b)–(c) that, TWI-ICLM achieves much better image quality compared to DBIM. Although DBIM can retrieved the outline of the unknown object roughly, there are lot artefacts in the background. In contrast, TWI-ICLM can well retrieve the profile and the value of permittivity. The corresponding quantitative evaluation metrics are summarized in Tab. 2.

Tab. 2 MSES/SSIM for the reconstructions in Fig. 6

Method	Test 4	Test 5
DBIM	0.118/0.600	0.134/0.620
TWI-ICLM	0.046/0.840	0.045/0.904

Consequently, it is shown that the proposed TWI-ICLM outperforms the traditional iteration method in TWI scenario. Despite the good results achieved, the TWI-ICLM can be further improved in credibility of predictions, such as by using advanced deep neural networks, or by further Incorporating physics theory into learning process.

5 Conclusion

In this work, we presented an induced current learning method, i.e., TWI-ICLM, to solve the inhomogeneous ISP for TWI scenario. The CNNs are designed to learn the induced current from initial results, which can significantly mitigate the nonlinearity and ill-posedness of the inverse problem. The proposed method has been verified with synthetic data and experimental data, and shows good potential in TWI applications including medical diagnostics and military surveillance.

References:

[1] M. G. Amin and F. Ahmad, *Academic press library in signal processing*, Amsterdam: Elsevier, 2014, pp. 857-909.

[2] J. A. Tobon Vasquez, R. Scapaticci, G. Turvani, M. Ricci, L. Farina, A. Litman, M. R. Casu, L. Crocco, and F. Vipiana, "Noninvasive inline food inspection via microwave im-aging technology: an application example in the food industry," *IEEE Antennas and Propagation Magazine*, vol. 62, no. 5, pp. 18-32, 2020.

[3] X. Song, M. Li, F. Yang, S. Xu, and A. Abubakar, "Study on joint inversion algorithm of acoustic and electromagnetic data in biomedical imaging," *IEEE Journal on Multiscale and Multiphysics Computational Techniques*, vol. 4, pp. 2-11, 2019.

[4] W. C. Chew and Y. M. Wang, "Reconstruction of two-dimensional permittivity distribution using the distorted Born iterative method," *IEEE Transactions on Medical Imaging*, vol. 9, no. 2, pp. 218-225, 1990.

[5] K. Xu, Y. Zhong, X. Chen, and D. Lesselier, "A fast integral equation-based method for solving electromagnetic inverse scattering problems with inhomogeneous background," *IEEE Transactions on Antennas and Propagation*, vol. 66, no. 8, pp. 4228-4239, 2018.

[6] Z. Wei and X. Chen, "Deep-learning schemes for full-wave nonlinear inverse scattering problems," *IEEE Transactions on Geoscience and Remote Sensing*, vol. 57, no. 4, pp. 1849-1860, 2019.

[7] Y. Liu, H. Zhao, R. Song, X. Chen, C. Li, and X. Chen, "SOM-net: unrolling the subspace-based optimization for solving full-wave inverse scattering problems," *IEEE Transactions on Geoscience and Remote Sensing*, vol. 60, pp. 1-15, 2022.

[8] T. Shan, Z. Lin, X. Song, M. Li, F. Yang, and S. Xu, "Neural Born iterative method for solving inverse scattering problems: 2D cases," *IEEE Transactions on Antennas and Propagation*, vol. 71, no. 1, pp. 818-829, 2023.

[9] X. Ye, Y. Bai, R. Song, K. Xu, and J. An, "An inhomogeneous background imaging method based on generative adversarial network," *IEEE Transactions on Microwave Theory and Techniques*, vol. 68, no. 11, pp. 4684-4693, 2020.

[10] Z. Wei and X. Chen, "Physics-inspired convolutional neural network for solving full-wave inverse scattering problems," *IEEE Transactions on Antennas and Propagation*, vol. 67, no. 9, pp. 6138-6148, 2019.

[11] M. Salucci, M. Arrebola, T. Shan, and M. Li, "Artificial intelligence: new frontiers in real-time inverse scattering and electromagnetic imaging,"

IEEE Transactions on Antennas and Propagation, vol. 70, no. 8, pp. 6349-6364, 2022.

[12] R. Guo, T. Huang, M. Li, H. Zhang, and Y. C. Eldar, "Physics-embedded machine learning for electromagnetic data imaging: examining three types of data-driven imaging methods," *IEEE Signal Processing Magazine*, vol. 40, no. 2, pp. 18-31, 2023.

[13] T. Zhou, F. Shen, Q. Meng, H. Li, K. Xu, D. Ye, J. Huangfu, S. Dong, T. A. Denidni, and L. Ran, "Towards real-time through-obstacle imaging based on compressed sensing for sparse objects," *IET Microwaves, Antennas & Propagation*, vol. 13, no. 13, pp. 2290-2296, 2019.

Pengjin Lan received the B.E. degree in communication engineering from Hezhou University, Hezhou, China, in 2019. He is currently working toward an M.S. degree with Faculty of Electrical Engineering and Computer Science, Ningbo University, Ningbo, China. His current research interests include learning-based inverse scattering problem and through-wall imaging.

Jianguo Huang received the B.E. degree in electronic information engineering from Taizhou University, Taizhou, China, in 2022. He is currently working toward an M.S. degree with Faculty of Electrical Engineering and Computer Science, Ningbo University, Ningbo, China. His current research interests in microwave inverse imaging.

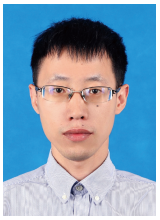

Tianyi Zhou received the B.S. and Ph.D. degrees in electrical engineering from Zhejiang University, Hangzhou, China, in 2013 and 2018, respectively. He became an assistant professor in 2018 and an associate professor in 2023, both with the Faculty of Electrical Engineering and Computer Science, Ningbo University, Ningbo, China. His current research interests include microwave imaging and wireless localization.